Space evaluation of 2048x1080 mirrors DMD chip for ESA's EUCLID Mission

Frederic Zamkotsian, Patrick Lanzoni, Emmanuel Grassi, Rudy Barette, Christophe Fabron, et al.

Frederic Zamkotsian, Patrick Lanzoni, Emmanuel Grassi, Rudy Barette, Christophe Fabron, Kyrre Tangen, Luca Valenziano, Laurent Marchand, Ludovic Duvet, "Space evaluation of 2048x1080 mirrors DMD chip for ESA's EUCLID Mission," Proc. SPIE 7731, Space Telescopes and Instrumentation 2010: Optical, Infrared, and Millimeter Wave, 773130 (10 August 2010); doi: 10.1117/12.861969

SPIE.

Event: SPIE Astronomical Telescopes + Instrumentation, 2010, San Diego, California, United States

Space evaluation of 2048x1080 mirrors DMD chip for ESA EUCLID mission

Frederic Zamkotsian[1], Patrick Lanzoni[1], Emmanuel Grassi[1], Rudy Barette[1], Christophe Fabron[1], Kyrre Tangen[2], Luca Valenziano[3], Laurent Marchand[4], Ludovic Duvet[4]

[1] Laboratoire d'Astrophysique de Marseille, CNRS, 38 rue Frederic Joliot Curie, 13388 Marseille Cedex 13, France
[2] Visitech, Kjellstadveien 5, Lier, P.O.Box 616, N-3003 Drammen, Norway
[3] INAF/IASF Bologna, via P. Gobetti 101, I-40129 Bologna, Italy
[4] European Space Agency, Keplerlaan 1, 2200 AG, Noordwijk, The Netherlands

E-mail address: frederic.zamkotsian@oamp.fr

ABSTRACT

Next-generation infrared astronomical instrumentation for ground-based and space telescopes could be based on MOEMS programmable slit masks for multi-object spectroscopy (MOS). This astronomical technique is used extensively to investigate the formation and evolution of galaxies.
We are engaged in an ESA study for a technical assessment of using a DMD from Texas Instruments for space applications (for example in ESA EUCLID mission). The DMD features 2048 x 1080 mirrors on a 13.68µm pitch, where each mirror can be independently switched between an ON (+12°) position and an OFF (-12°) position. For MOS applications in space, the device should work in vacuum, at low temperature, and each MOS exposure would last for typically 1500s with micromirrors held in a static state (either ON or OFF). A specific thermal/vacuum test chamber has been developed for test conditions down to -40°C at 10^{-5} mbar vacuum. Imaging capability for resolving each micromirror has also been developed for determining degradation in any single mirror. Our first tests reveal that the DMD remains fully operational at -40°C and in vacuum. A 1038 hours life test in space conditions, Total Ionizing Dose radiation, thermal cycling and vibrations/shocks have also been successfully completed. These results do not reveal any concerns regarding the ability of the DMD to meet environmental space requirements.
We have also developed a bench for MOS demonstration using MOEMS devices. DMD chip has been successfully tested revealing good contrast values as well as good functionality for applying any mask pattern, demonstrating its full ability for space instrumentation, especially in multi-object spectroscopy applications.

Keywords: micromirror array, space evaluation, multi-object spectrograph, EUCLID mission, MOEMS.

1. INTRODUCTION

Next-generation infrared astronomical instrumentation for ground-based and space telescopes could be based on MOEMS programmable slit masks for multi-object spectroscopy (MOS). This astronomical technique is used extensively to investigate the formation and evolution of galaxies. The EUCLID mission from the European Space Agency (ESA) will study the dark universe by characterizing a very high number of galaxies in shape and in spectrum. In order to optimize the Signal-to-Noise Ratio (SNR) value, the high precision spectra measurements could be obtained via multi-object spectroscopy (MOS). Multi-object spectroscopy (MOS) with multi-slits is the best approach to eliminate the problem of spectral confusion, to optimize the quality and the SNR of the spectra, to reach fainter limiting fluxes and to maximize the scientific return both in cosmology and in legacy science. Major telescopes around the world are equipped with Multi-Object Spectrographs (MOS) in order to simultaneously record several hundred spectra in a single observation run. Next generation MOS for space like the Near Infrared Multi-Object Spectrograph (NIRSpec) for the James Webb Space Telescope (JWST) require a programmable multi-slit mask. Conventional masks or complex fiber-optics-based mechanisms are not attractive for space. The programmable multi-slit mask requires remote control of the multi-slit configuration in real time.

A promising possible solution is the use of MOEMS devices such as micromirror arrays (MMA) [1,2,3] or micro-shutter arrays (MSA).[4] MMAs are designed for generating reflecting slits, while MSAs generate transmissive slits. MSA has

Space Telescopes and Instrumentation 2010: Optical, Infrared, and Millimeter Wave, edited by Jacobus M. Oschmann Jr., Mark C. Clampin, Howard A. MacEwen, Proc. of SPIE Vol. 7731, 773130 · © 2010 SPIE · CCC code: 0277-786X/10/$18 · doi: 10.1117/12.861969

been selected to be the multi-slit device for NIRSpec and is under development at NASA's Goddard Space Flight Center. They use a combination of magnetic effect for shutter actuation, and electrostatic effect for shutter latching in the open position. In Europe, an effort is currently under way to develop single-crystalline silicon micromirror arrays for future generation infrared multi-object spectroscopy.[5, 6] By placing the programmable slit mask in the focal plane of the telescope, the light from selected objects is directed toward the spectrograph, while the light from other objects and from the sky background is blocked. For example, a MOEMS-based MOS concept where the programmable slit mask is a MMA is shown in the left-hand side of Fig. 1. In action, the micro-mirrors in the ON position direct the light toward the spectrograph and appear bright, while the micro-mirrors in the OFF position are dark.

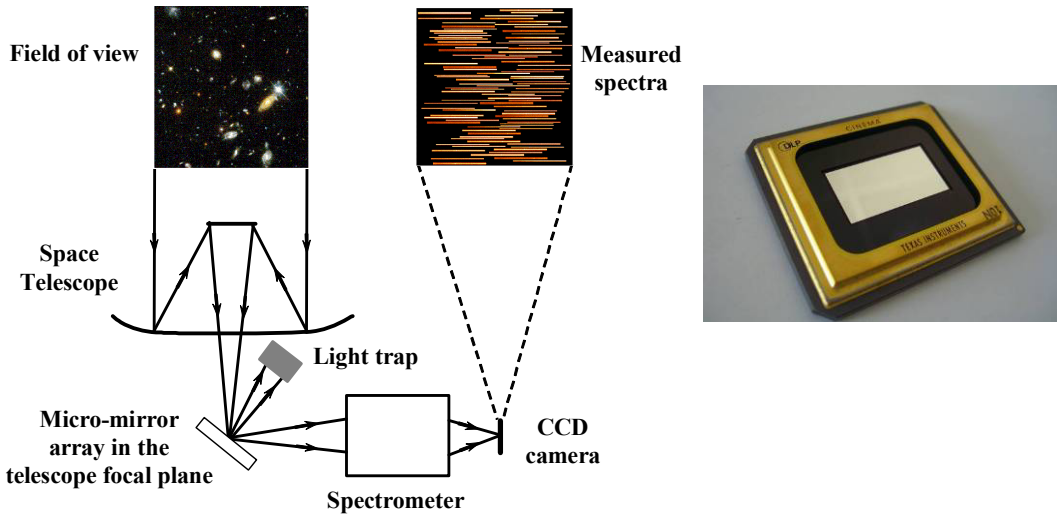

Fig. 1: Principle of a Multi-Object Spectrograph with a Micro-Mirror Array.
DMD chip from Texas Instruments (2048 x 1080 micromirrors).

In the timescale of the EUCLID mission, a specialized programmable multi-slit mask cannot be developed. This component has to be commercially available. To get more than 2 millions independent micromirrors, the selected component for an EUCLID pre-study is a DMD chip from Texas Instruments that features 2048 x 1080 mirrors and a 13.68µm pixel pitch (right-hand side of Fig. 1). Typical operational parameters are room temperature, atmospheric pressure and mirrors switching thousands of times in a second, while for EUCLID, the device should work in vacuum, at low temperature, and each MOS exposure lasts between 400s and 1500s, with mirrors held in one state (either ON or OFF) during the exposure.

Visitech is an engineering company experienced in developing DMD solution for industrial customers. The Laboratoire d'Astrophysique de Marseille (LAM) has, over several years, developed different tools for modeling and characterization of MOEMS-based slit masks, especially during the design studies on JWST-NIRSpec. [7, 8] ESA has engaged with Visitech and LAM in a technical assessment of a DMD chip for space application. A specific thermal / vacuum test chamber has been developed for test conditions down to -40°C at 10^{-5} mbar vacuum. Imaging capability for resolving each micro-mirror has also been developed for determining any single mirror failure. Dedicated electronics and software allows us to hold any pattern on the DMD for duration of up to 1500s.

We present the summary of this ESA study, the electronic test vehicle as well as the cold temperature test set-up we have developed. Then, results of tests in vacuum at low temperature, including low temperature stress test, low temperature nominal test, thermal cycling, and life test are presented. Results after radiation (TID and proton), and vibration and shock are also shown. Finally MOS-like tests have been done.

2. THE ELECTRONIC TEST VEHICLE

This paragraph provides a description of the electronic test vehicles. The first section describes some of the specific requirements that the test vehicles had to fulfill, the next section explains the details on how the various modes of the DMD were created and the last section deals with a brief description of the main parts of the electronic test vehicles.

2.1 Architecture of the electronic test vehicles

The DMD driver electronics consists of a formatter board and a DMD board. The general architecture of the system is described in Figure 2. There is a notable difference that separates this system from other DMD board designs; the control signals of the DAD1000 reset drivers are fed through an FPGA. This enables splitting the DMD into five zones with each zone being driven with a different pattern and refresh rate. This functionality reduces the number of test vehicles and test duration because several conditions can be tested in parallel on the same DMD. An explanation of the functionality can be found in paragraph 3.2. The following is a brief description of the building blocks of the system

Formatter board, RS232 input: The input enables control of the formatter board from a PC.

Formatter board, DVI input: The input receives test images from a PC and transfer them to the FPGA.

Formatter board, FPGA: 1) The integrated micro controller handles RS232 communication and programs the DDP1000 formatters. 2) The signals from the DVI input are processed before being sent to the DDP1000 formatters. 3) Manipulation of the DAD1000 reset drivers control signals, details can be found in paragraph 5.

Formatter board, DDP1000: The two DDP1000 formatters handle DMD image processing. Each formatter has a corresponding RAMBUS memory.

DMD board: The DMD board contains the DMD and two DAD1000 reset drivers.

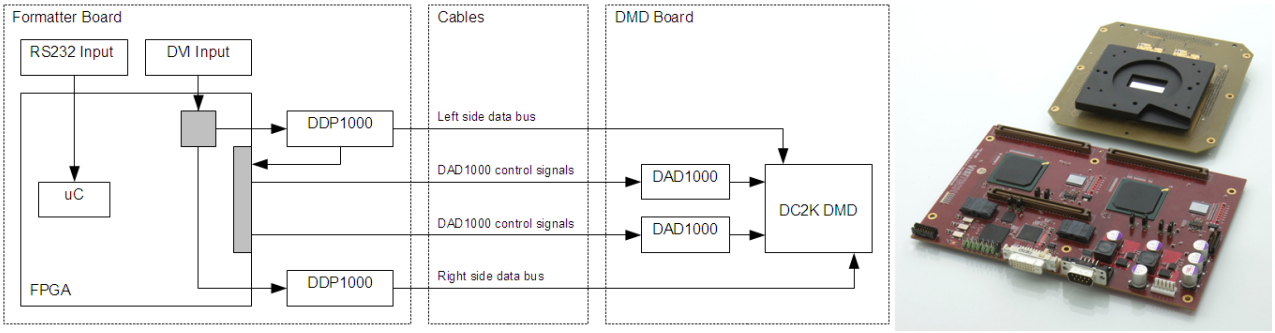

Fig. 2: Block diagram and pictures of the formatter and DMD board.

2.2 Environmental requirements for the electronic test vehicles

The electronic test vehicles were designed by Visitech for extreme test conditions using essentially commercial off the shelf components. In addition, the EUCLID operation requires that each DMD micromirror will be held in one position for 1500 seconds at a time. The budget and schedule of the EULID pre-study meant that compromises had to be made, and the following describes some of the compromises and how we minimized risk and potential impact to the budget and schedule.

Low temperature operation: Except for the DMD, DDP1000, DAD1000 and the RAMBUS memory, the system uses commercial off the shelf components, which can operate at -40°C.

Vacuum operation: The DMD board has no protective coating or printed reference designators that can cause outgassing. All components on the DMD board were selected in an attempt to avoid outgassing materials.

Radiation testing: Careful layout of the components on the electronics boards allowed for efficient shielding of active components that should not be radiation tested. Current sense resistors enabled current measurements during and in between radiation testing.

3. COLD TEMPERATURE TEST EQUIPMENT AND PROCEDURE

The Laboratoire d'Astrophysique de Marseille has over the last few years developed an expertise in the characterization of micro-optical components. [8,9,10] This expertise in small-scale surface deformation characterization of micro-optical components as well as operational testing of MOEMS components has been used for developing a dedicated cold temperature test set-up for DMD measurements in EUCLID operating conditions.

3.1 Cryostat & optical bench

For environmental testing (vacuum and low temperature), a cryostat has been developed at LAM. The bench (Fig. 3) is used as a photometric bench. In order to get enough resolution on each micromirror, the FOV images approximately

200x200 micromirrors onto a 1k x 1k camera. To inspect the complete DMD, a stitching procedure is carried out, by means of motorized stages. For the sake of test accuracy and efficiency, the characterization set-up is automated as much as possible. Three computers are used for managing the tests. The thermal chamber enables tests in a vacuum environment with temperature adjustment in the range of -60°C to +20°C. Temperature change is obtained through a liquid cooler. The chamber is made of a stainless steel cross. Each side is devoted to a specific task. The first side includes a window in order to view the DMD sample; the second side holds the feed-through connectors for driving the DMD board; the third side permits all sensing wires (for temperature sensors) to pass into the chamber. Finally, the fourth side receives the pipes from the liquid cooler device. The cryostat is monitored with temperature sensors and vacuum sensors driven by a computer (*cryostat computer* in Fig. 3). Illumination of the DMD array is made by a collimated beam. Optical imaging is made by two doublets (200mm – 400mm) mounted on rail. The system is diffraction limited on the detector, leading to an optimized photometric measurement. The device is divided into **50 zones**. The FOV to be imaged by the CCD camera covers one zone, equivalent to **205 x 216 micromirrors** (44280 micromirrors). The plate scale on the 1k x 1k camera is exactly 4.07 x 4.07 detector pixels / micromirror. For complete DMD testing, the stitching procedure is done by means of motorized stages in three directions (XYZ), with a travelling range of 100mm and a resolution of 0.1µm. The optical test equipment (stages + camera) are monitored by a computer (*test computer* in Fig. 3). All software is developed in Matlab.

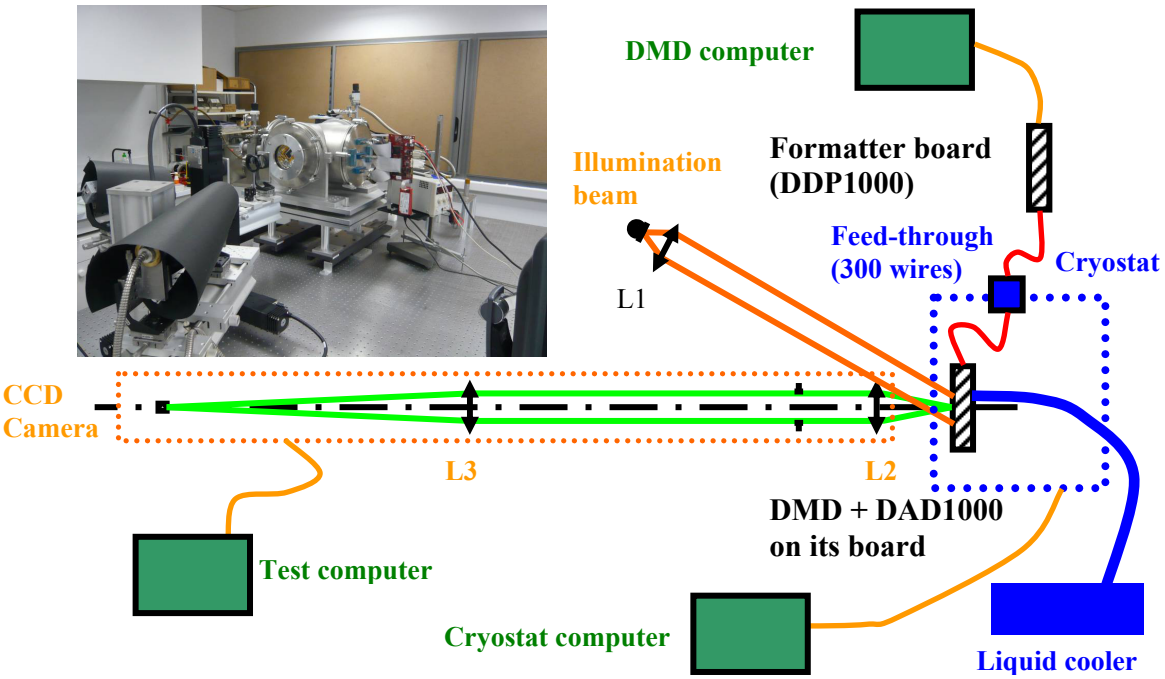

Fig. 3: Cold temperature test set-up

The DMD board is mounted on the thermal interface through a point-plane-plane mounting scheme in order to avoid any additional stress on the board when the temperature is changing. The thermal link between the thermal interface and the DMD board as well as the DMD itself is done through copper wires connected to the DMD board, the DMD heat sink and the front mounting surface of the DMD device (Fig. 6, left-hand image). The DMD board is linked by 300 wires through the chamber to the formatter board. Specialized feed-throughs for such high number of wires has been realized, tested, and have been mounted on our chamber. All materials used in the chamber are vacuum compatible, except the wires leading to the DMD board and some parts on the DMD board. After DMD board integration, the thermal screen with Multi-Layer Insulator (MLI) cover is mounted around the device, and the optical window is closed on the chamber. We have decided to align and fix the optical input and output beams as a very precise and reliable reference. Then all optical alignments are performed on the chamber, using the tip-tilt and rotation mounting under the cryo chamber. When the DMD chip and the detector are in parallel planes, the stitching of the images could be done much easier with the motorized stages moving the optical train. A focused image across the whole device is maintained

without the need for Z stage adjustment during stitching with the X and Y stages. By this way, the optical input and output beams stay fixed with respect to the DMD.

3.2 Device driving

Hardware and software were developed by Visitech and LAM for driving the DMD boards. The hardware is controlled by a RS-232 serial link and a DVI port is used for loading an image onto the DMD. The software is developed in Matlab for driving the DMD chip by a computer (*DMD computer* in Fig. 3).

In addition to the extreme conditions of a EUCLID environment, this DMD-based instrument also has a very non-typical DMD operation: during data capture, each DMD micromirror will be held in one position for 1500 seconds before changing state. This is quite a challenge to accomplish with a DDP1000 based chip set and testing is required in static ON and static OFF modes in addition to normal display-type operation. Normal display-type operation is used as a base line in analyzing test results. Schedule of the ESA activity did not allow for testing static and normal display-type modes on separate devices. To meet all requirements, each DMD has been divided into 5 horizontal rows and each row can be driven in normal display-type mode or static modes (Fig. 4). This allows for testing of all modes on a single DMD at the same time. 4/5 of the DMD operates in a static ON or OFF mode (arbitrary pattern) and 1/5 of the DMD operates in display-type mode where the pattern is updated at 1Hz rate. This results in a display-type zone of roughly 400 000 micromirrors and static zones of 4 times this size, which is an ample amount for statistical analysis of the test results.

The two major patterns, pattern 1 and pattern 2, are designed as “positive” and “negative” to each other (Fig. 4). Each pattern row is divided in 10 zones for a total of 50 zones, and each zone is imaged on the CCD camera. Each zone includes specific patterns identical from zone to zone and numbers at the edge of each zone are set for easy processing and archiving (central picture of Fig. 4). The individual patterns show lines with different width and orientation, chessboard features and MOS-like patterns. In addition to pattern 1 and pattern 2, all ON and all OFF mirrors will also be displayed and measured at each measurement step. Background will be measured and subtracted from the images.

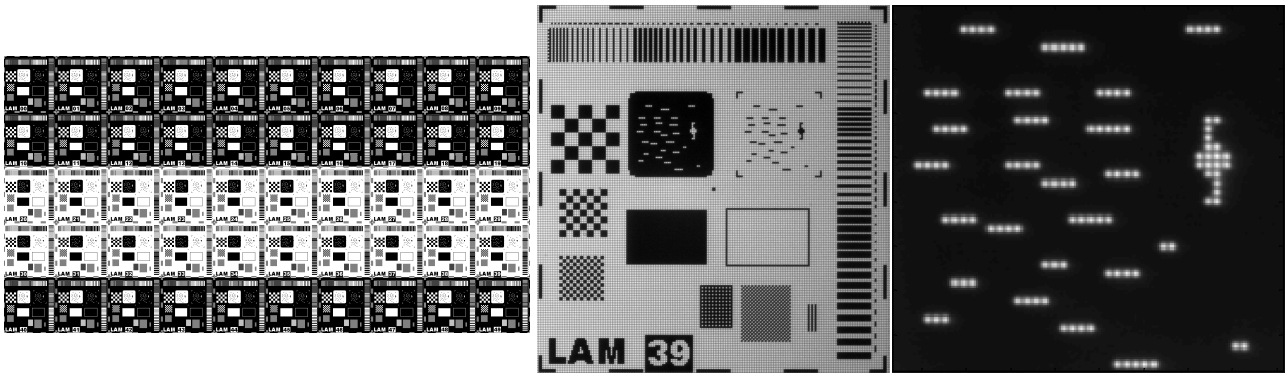

Fig. 4: LAM designed pattern (pattern 1); Image of a zone taken with the characterization set-up CCD camera and close-up view on a MOS-like pattern

Each micromirror is imaged on the CCD camera on about 4x4 detector pixels, which is enough for monitoring and detection of failures (if any) during the tests. A zoom on the area simulating a MOS-like pattern, with multi-slits is shown in right-hand side of Fig. 4. Any slit location and shape can be generated. It has to be noticed that the OFF mirrors cannot be imaged on the detector due to the high contrast performance of DMD. Then, the contrast cannot be measured in this test. An evaluation of the contrast will be done during the MOS-like tests, using a high dynamical range camera.

3.3 Analysis procedure

A data pipeline for data reduction has been developed using Matlab software. Photometric measurements are done before, during and after each test, and compared to the reference measurements (taken before the test, at room temperature). Any degradation in performance of a mirror will be revealed. Differences between mirrors as well as tests on different patterns applied on the same device (patterns in space domain and time domain) will be analyzed. The analysis procedure comprises background subtraction, patterns recentering, mirrors detection, comparison with the nominal mirror photometric measurement; local variations of the illumination beam are taken into account. We have

adopted three mirror degradation definitions: - the **blocked mirror** when the mirror is non-responsive (e.g. "stuck"), - the **lossy mirror** when the optical throughput is decreased by more than 20%, and – the **weak mirror** when the optical throughput is decreased between 10% and 20%. Typical images of these types of mirrors are shown in Fig. 5 (central mirror in each image). Blocked mirrors show a lack of light on the micro-mirror area, while for lossy and weak mirrors, a decrease in the throughput is observed. For automatically detecting these mirrors, we have defined two parameters: **micro-mirror average throughput calculation** and **centroid calculation**. The micro-mirror average throughput is the flux integrated in the area of each micro-mirror. The centroid is calculated within the area of the micro-mirror and located on the map, as displayed in Fig. 5. For blocked mirrors, there is a major shift while for lossy mirrors, the shift is small. There is nearly no shift for weak mirrors.

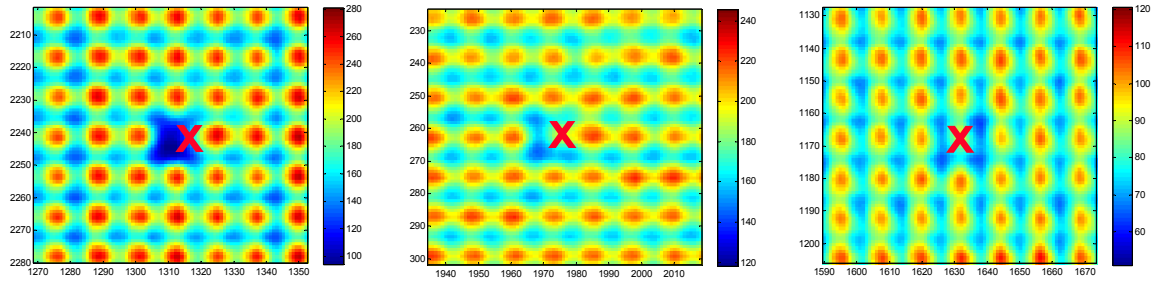

Figure 5: Three types of mirrors with failure: blocked, lossy and weak; centroid locations are marked with an "x".

We have developed software for an automatic analysis of all data recorded during our measurements. All failure types are searched and detected. Results are displayed into maps and graphs. In some cases, the mirrors could appear with an extra-brightness (extra-throughput in the range + 10% to 20%). After the first analysis process, a second level of analysis is done: we name it as a cleaning process, for removing false failure detections. The false failure detections are due mainly to dust particles present on the camera or the DMD window. Dust on the camera is revealed by failure detection located in the same area for each zone, while dust on the DMD window will appear in the same place on the DMD from measurement to measurement. Some mirrors flagged as affected could be false detection due to very small dust particles, but this effect could affect only marginally the weak mirrors. The final results are then given in three graphs (example: Fig. 7) showing the number and the locations of failed mirrors (blocked, lossy and weak). All fifty zones from the DMD are shown in a matrix pattern (zone 00 to zone 49), and the number of affected mirrors is assigned to each zone. Comparison of measurements before and after testing shows the evolution of the failure rate.

4. COLD TEMPERATURE TEST

Four sets of cold temperature tests have been completed: cold temperature step stress test, nominal cold temperature test, thermal cycling and life test. Pictures of the device mounted in the chamber during life test in LAM's cold chamber are shown in Fig. 6.

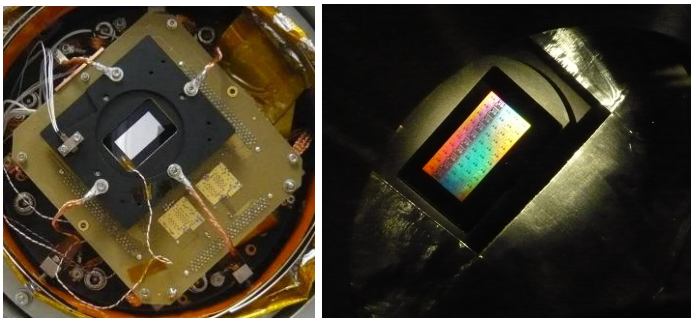

Fig. 6: Pictures of the device during life test.

4.1 Cold temperature step stress test and nominal cold temperature test

The cold temperature step stress test has been done from room temperature down to -60°C. **This test shows that permanent failure, i. e. stuck mirrors, is appearing on some mirrors when the device is taken down to -55°C.** The failure rate increases at -60°C.

Based on these results, the nominal temperature condition for EUCLID was set to -40°C. In order to confirm that this is an acceptable nominal operating condition for the device, a single DMD was tested. The DMD was mounted in the cold temperature chamber and tested three times at this temperature. For minimizing stress on the device when cooling down, a fast (-40°C / hour) and homogeneous cooling was provided. Using the definitions of blocked, lossy and weak mirrors, we have analyzed all (over 2 million) mirrors from the DMD for each measurement. No blocked mirror was revealed while only 12 mirrors are defined as lossy, and between 3 to 7 as weak mirrors. According to the screening procedure of TI where all mirrors are considered to be either working or not working, this measurement shows intermediate states where lossy and weak mirrors are observed; lossy mirrors stay lossy during the whole test, and weak mirrors may change in status from test to test; all other mirrors show their full performances. This effect is possibly due to local non-uniformity at individual mirror level, present since device fabrication. We highlight the fact that these effects have no impact in a typical DMD display mode, but they have to be taken into consideration and calibrated for MOS application. These numbers are very low when compared to the total 2 millions mirrors operating in the device.

This test revealed no degradation of the device when three consecutive cycles in EUCLID conditions are applied. The cold temperature step stress test and the nominal cold temperature test have been fully described previously. [11]

4.2 Thermal cycling

Thermal cycling has been done on one DMD mounted on a DMD board, and conducted at INAF/IASF's facility in Bologna in Italy, and first five cycles as well as the optical characterizations have been performed at LAM's facility in Marseille in France. An Angelantoni ACS Challenger 250 Climatic chamber located in a class 100.000 clean room was used for the 562 thermal cycles conducted at INAF/IASF. Two sets of cycles (249 and 313 cycles) have been applied, with intermediate and final optical characterization.

No anomaly was observed on the DMD by visual inspection with unaided eye after the thermal cycling was completed but some dirt was deposited on the DMD window during cycling. In particular no cracks, no flakes were observed. The results for the reference measurement at +20°C are presented in Fig. 7 first row in three graphs showing the number and the locations of affected mirrors with 1 blocked, 4 lossy, and 15 weak mirrors. The results for the measurement at -40°C after the first serial of 254 cycles are given in Fig. 7 second row with 1 blocked, 2 lossy, and 7 weak mirrors. The results for the third measurement at -40°C after the second serial of 313 cycles are shown in Fig. 7 third row with 0 blocked, 6 lossy, and 30 weak mirrors.

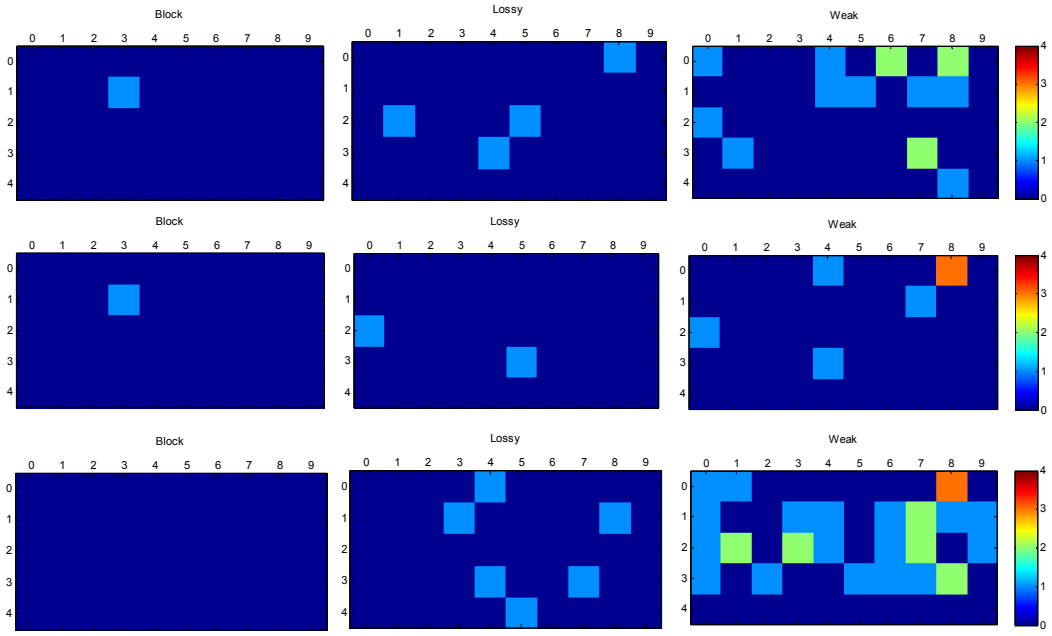

Fig. 7: First row: Location and numbers of affected mirrors at +20°C.
Second row: Location and numbers of affected mirrors at -40°C, after the first serial of 254 cycles.
Third row: Location and numbers of affected mirrors at -40°C, after completion of all cycles (567 cycles).

Either one or zero blocked mirror is observed during this test, located in zone 13. The measured throughput is at the limit between blocked and lossy mirror. Between two and six lossy mirrors have been observed during the thermal cycling test: for most of them, they are located in different places, these mirrors being at the limit between lossy and weak mirrors. The number of weak mirrors is in the same range before and after testing; a slight increase of this number could be due to the extra dirt on the window. From these charts, we clearly see that the same behavior is occurring for mirrors switching frequently (display mode in the central row) or in a static pattern during 1500s (EUCLID mission conditions), in the four other rows.
In conclusion of the thermal cycling, this test has been successfully completed. This shows that space conditions did not degrade the device performances, within this thermal cycling campaign.

4.3 Life test

The life test has been completed on one DMD device. The device was tested in EUCLID conditions, this means in vacuum, at -40°C and the device was operating with the following test cycle: pattern 1 is applied for 1500s (central pattern row is tilting in display mode while other pattern rows display a static pattern), the whole device is switching between pattern 1 and pattern 2 for 60s and pattern 2 is applied for 1500s (central pattern row is tilting in display mode while other pattern rows display a static pattern). By this way, there is an identical duty cycle for all mirrors. **The life test lasted for 1038 hours.** Full optical tests were done during the whole life test. Measurements were done at room temperature (reference measurement), a first test at cold temperature was done at T0, then 11 intermediate measurements were done, and finally, a last measurement was done at the end of the life test, after **1038h.**

During the whole test, the DMD operational temperatures were recorded:

- DMD heat sink temperature (close to the actual DMD component temperature point): **-41°C**
- DMD front mounting surface temperature: **-36°C**
- Thermal interface temperature: **-49°C**

We can note that when the DMD is turned off, a drop of **2-3°C** in temperature is revealed, showing the heating capability of the DMD chip due to its power consumption.

After recording all data, we used the analysis procedure described in paragraph 3 for extracting the number and the locations of affected mirrors (blocked, lossy, weak). The results for the reference measurement at +20°C are presented in Fig. 8 first row in three graphs showing the number and the locations of affected mirrors with 3 blocked, 7 lossy, 12 weak mirrors. The results for the last measurement at -40°C after 1038 hours of operation are shown in Fig. 8 second row with 3 blocked, 7 lossy, 8 weak mirrors. All intermediate tests are identical to these results with very little variation of only few mirrors for the weak case. From these charts, we clearly see that the same behavior is occurring for mirrors switching frequently (display mode in the central row) or in a static pattern during 1500s (EUCLID mission conditions), in the four other rows.

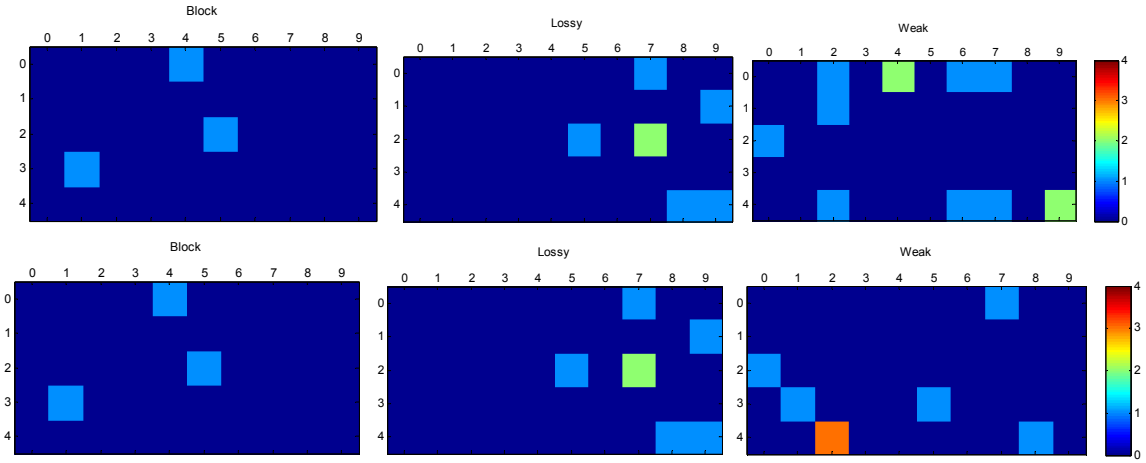

Fig. 8: First row: Location and numbers of affected mirrors at +20°C.
Second row: Location and numbers of affected mirrors at -40°C, after 1038 hours of life test.

In conclusion of the life test, this test has been successfully completed. Three blocked mirrors and five lossy mirrors have been observed, but they are detected at ambient, at cold temperature at the beginning of the test and at cold temperature at the end of the test; they are not a consequence of the space conditions applied to the device. Other affected mirrors are only weak mirrors and their number is very low, with no increase while the life test is running. **This shows that space conditions did not degrade the device performances, within this life test period.**

5. TID AND PROTON SEE RADIATION TESTING

5.1 Total Ionizing Dose (TID) test

A complete test vehicle had to be in operation during the radiation testing, but by carefully shielding the test vehicle with lead bricks, only selected devices received a significant radiation dose. The devices to be irradiated were selected in such a way that the artifacts of a failing device would help in pinpointing which device had failed. The devices to be irradiated were the DMD, one DDP1000, one RAMBUS memory and one DAD1000. During the radiation testing the DMD displayed full black and full white test patterns that alternated every 1500 seconds. This is similar to the expected EUCLID duty cycle. A data logger measured the current consumption of major power supplies of the DMD chip set during radiation and provided the opportunity to monitor if and when any of the devices were degrading. **Total Ionizing Dose (TID) radiation tests established a tolerance level of 10 - 15 Krads for the DMD; at mission level, this limitation could likely be overcome by shielding the device.** The TID test has been fully described previously. [11]

Optical characterizations were done on the samples before and the day after the radiation. An additional test was carried out one week later in order to measure longer term effect. No blocked mirror and five lossy mirrors have been observed before and after TID radiations; all lossy mirrors being at the same location. Other affected mirrors are weak mirrors and their number is low (around 30 mirrors), with no increase after the test. **We can then conclude that these results show that space conditions did not degrade the device performances, within this TID radiations test conditions.**

5.2 Proton Single Event Effects (SEE) radiation test

The proton radiation test has been performed at the KVI facility in the Netherlands. During proton radiation, a live optical characterization has been conducted on a limited FOV around the center of the radiation beam hitting the device. The proton beam has an angle of around 45° with respect to the DMD surface, and the beam is located precisely on the DMD surface thanks to a laser guiding beam provided on the KVI equipment. The optical set-up is based on the set-up used in Marseille with a collimated input beam (LED) and an imaging system with two doublets, giving the right magnification on the camera for observing the individual micro-mirrors with enough spatial resolution.

The conditions for the first run was a 48 MeV beam from the accelerator, leading to 34.7 MeV on the DMD after crossing the DMD window at 45°. The radiation started at low flux (6 10^5 p/cm^2/s for 300s) and was to be increased to a higher flux (5 10^7 p/cm^2/s for 896s) in order to reach a total dose of 10 Krads on the DMD. The proton radiation testing was unfortunately ended prematurely because of a break down in the accelerator after 120 seconds of radiation at low flux. **The lack of observed single events upsets is promising, but considering the length of the test, no conclusions can be made on the tolerance of the test vehicle in regards to single events upsets.**

6. VIBRATIONS AND SHOCKS

6.1 Vibration testing

Mechanical vibration testing has been done on one DMD, and was conducted at ESTEC's facility in Noordwijk, the Netherlands. For this test, the standards MIL-STD-883F, methods 2005 (vibration fatigue) and 2007 (vibration at variable frequency) condition A, are followed: 20g during 32hours on each axis for vibration fatigue, and 20g at 20-2000Hz, 4 times on each axis for vibration at variable frequency. For both vibration tests, the set-up is a lab shaker and a support for the device. A control accelerometer is fixed on the support and the acceleration profile during the vibration testing is monitored. A special frame was manufactured to hold the DMD during the test and a double sided tape was used as an interface between the aluminium support and the ceramic package of the device which is very brittle. The vibration testing resulted in no visual effects that could be seen on the tested devices.

The optical characterizations have been performed at LAM's facility in Marseille in France. After recording all data, we used the analysis procedure described in paragraph 3 for extracting the number and the locations of affected mirrors (blocked, lossy, weak). The results for the reference measurement at +20°C, before vibrations, are presented in Fig. 9 first row in three graphs showing the number and the locations of affected mirrors with 0 blocked, 2 lossy and 8 weak mirrors. The results after vibrations, at -40°C, are shown in Fig. 9 second row with 0 blocked, 1 lossy and 9 weak mirrors. No blocked mirror and one lossy mirror have been observed before and after vibrations (at -40°C after vibrations). A second lossy mirror before vibrations is no longer visible after vibrations. Other affected mirrors are weak mirrors and their number is very low, with no increase after the test. **This shows that space conditions did not degrade the device performances, within this vibrations test conditions.**

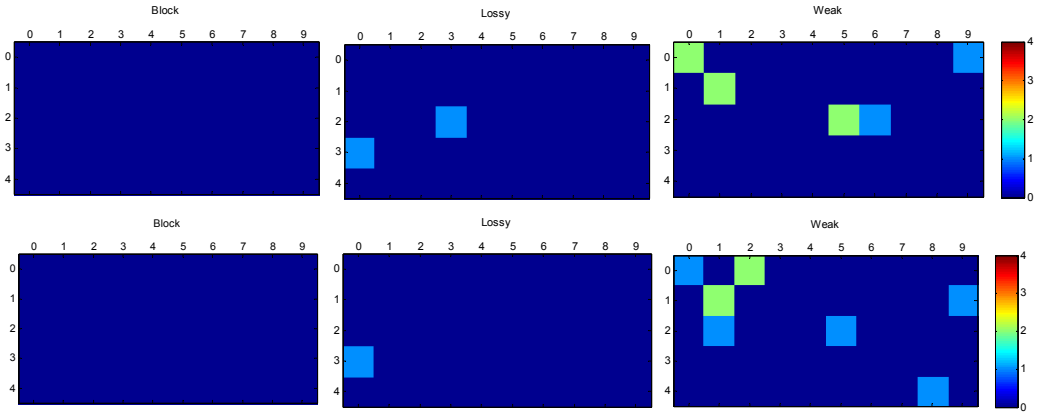

Fig. 9: First row: Location and numbers of affected mirrors at +20°C, before vibrations.
Second row: Location and numbers of affected mirrors at -40°C, after vibrations.

6.2 Shocks testing

Mechanical shock testing has been done on one DMD, and was conducted at ESTEC's facility in Noordwijk, the Netherlands. Shock test condition B of the MIL-STD-883f Method 2002 was applied on one DMD during shock testing. It consists of a shock with a peak acceleration of 1500g and pulse duration equal to 0.5ms, 5 times on each axis. The device is fixed on a mass which is dropped in free fall against a stopper. A control accelerometer is fixed on the support and the acceleration profile during the shock is monitored. A special frame was manufactured to hold the DMD during the test and a double sided tape was used as interface between the aluminium support and the ceramic package of the device which is very brittle. The shock testing resulted in no visual effects that could be seen on the tested vehicles. The optical characterizations have been performed at LAM's facility in Marseille in France. After recording all data, we used the analysis procedure described in paragraph 3 for extracting the number and the locations of affected mirrors (blocked, lossy, weak). The results for the reference measurement at +20°C (before shocks) are presented in Fig. 10 first row in three graphs showing the number and the locations of affected mirrors with 0 blocked, 3 lossy and 7 weak mirrors. The results after shocks, at -40°C, are shown in Fig. 10 second row with 0 blocked, 3 lossy and 6 weak mirrors.

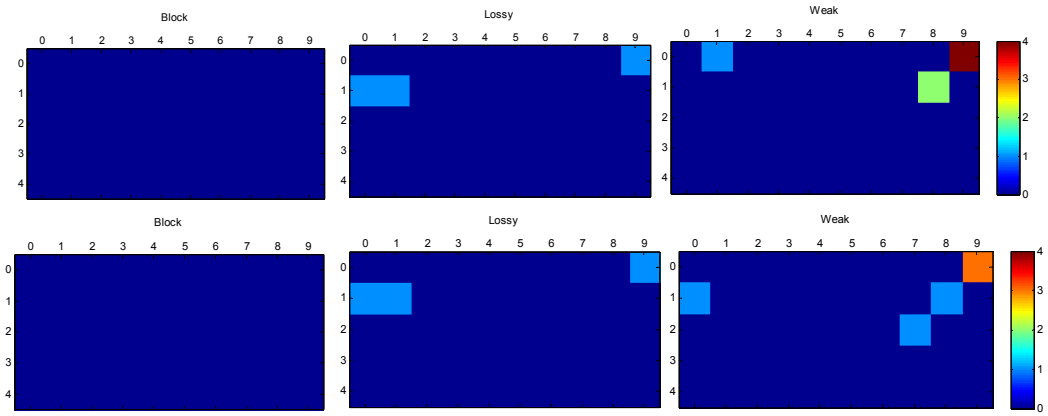

Fig. 10: First row: Location and numbers of affected mirrors at +20°C, before shocks.
Second row: Location and numbers of affected mirrors at -40°C, after shocks.

No blocked mirror and three lossy mirrors have been observed before and after shocks (at -40°C after shocks), at the same locations. Other affected mirrors are weak mirrors and their number is very low, with no increase after the test. **This shows that space conditions did not degrade the device performances, within this shock test conditions.**

7. MOS-like TESTS

In order to evaluate the capability of a DMD device to select objects in a field of view, we have developed a dedicated test set-up, demonstrating the concept of a DMD-based MOS spectrograph. From a field of view simulator, objects could be selected with the DMD device. Then, device performances have been measured and object selection procedure has been evaluated.

For the MOS test, an optical characterization test setup has been developed at LAM. The bench is used as a photometric bench, and the FOV is imaged on a 1kx1k camera in order to get enough resolution on each micro-mirror. Each micro-mirror is imaged on about 9 x 9 detector pixels. In comparison with the set-up developed for vacuum and low temperature testing (4 x 4 detector pixels / micro-mirror), the optical magnification is higher in this new set-up; we want then to get a higher photometric accuracy in DMD performance parameters, as well as a higher spatial resolution on each micro-mirror. We set a 24° angle between input and output beam, and both input and output beam have been set to F/3. In front of the camera, we are able to introduce a neutral density filter in order to increase the dynamical range of the bench, this feature is very important for the precise DMD contrast determination.

A FOV containing three objects was imaged on the DMD device surface (Fig. 11 a). In Fig. 11 b, the same FOV is presented, but the DMD is programmed in order to select the left-hand object (the mirrors are ON only on the object to be selected, and the rest of the mirrors are OFF). **This picture shows the full capability of the DMD device to generate any slit pattern (reflective slit) sending the light towards the spectrograph, when all other sources as well as background are hidden by the OFF micro-mirrors.** The contrast of a micro-mirror is defined as the ratio of the throughput when the mirror is in ON position with respect to the mirrors in OFF position. In order to be as accurate as possible, the throughput is integrated within a mask applied on a whole micro-mirror. The background light has been removed. **This gives a final value of the contrast of 2250.** Contrast has been measured on several mirrors and they exhibit identical values.

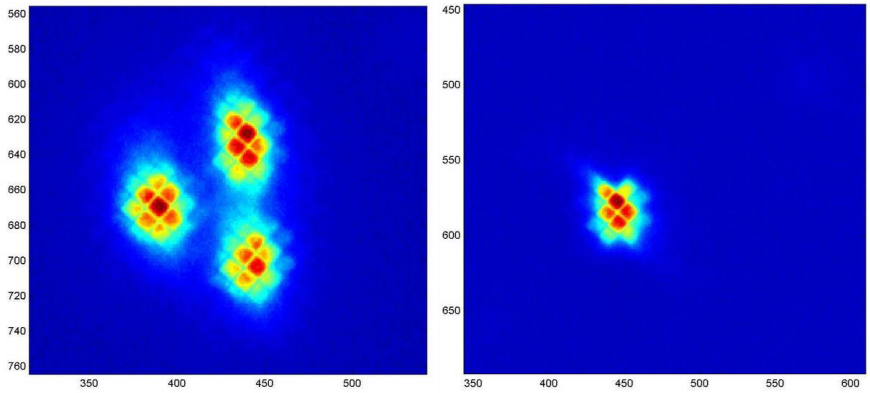

Fig. 11: (a) FOV with three objects imaged on the DMD device surface. (b) Same FOV when the DMD is programmed in order to select the left-hand side object (the mirrors are ON only on the object to be selected, and the rest of the mirrors are OFF).

8. CONCLUSION

Large field of view surveys with a high density of objects such as high-z galaxies or stars, such as in ESA EUCLID mission, benefit of multi-object spectroscopy (MOS) technique. Digital Micromirror Devices (DMD) could act as objects selection reconfigurable mask. ESA has engaged with Visitech and LAM in a technical assessment of using a DMD from Texas Instruments (2048 x 1080 mirrors on a 13.68µm mirror pitch) for space applications. Specialized driving electronics and a cold temperature test set-up have been developed.

Our tests reveal that the DMD remains fully operational at -40°C and in vacuum. The 1038 hours life test in space survey conditions (-40°C and vacuum), has been successfully completed. The device was operating continuously with typical MOS patterns. The numbers of affected mirrors are very low compared to the 2 million mirrors of the DMD array. Total Ionizing Dose (TID) radiation tests established a tolerance level of 10 - 15 Krads for the DMD; at mission level, this limitation could likely be overcome by shielding the device. Finally, thermal cycling (over 500 cycles between room temperature and cold temperature, on a non-operating device) and vibration and shock tests have also been done; no degradation is observed from the optical measurements.

These results do not reveal any show-stopper concerning the ability of the DMD to meet environmental space requirements. Insertion of such devices into final flight hardware would still require additional efforts such as development of space compatible electronics, and original opto-mechanical design of the instrument.

From an ESA perspective, the micromirror arrays have therefore achieved a reasonable TRL (Technology Readiness Level). Insertion of such devices into final flight hardware would still require additional efforts (estimation is approximately 2 years) in terms of change of the window coating, re-development of space compatible electronics as well as a different package interface compatible with spacecraft launch conditions.

ACKNOWLEDGEMENT

The authors thank Jean-Antoine Benedetti, Philippe Laurent and Vincent Herault from LAM for their assistance during the tests. This work is partly funded by ESA, CNRS, Provence-Alpes-Cote d'Azur regional council and Conseil General des Bouches-du-Rhone county council.

REFERENCES

1. R. Burg, P.Y. Bely, B. Woodruff, J. MacKenty, M. Stiavelli, S. Casertano, C. McCreight and A. Hoffman, "Yardstick integrated science instrument module concept for NGST", in *Proceedings of the SPIE conference on Space Telescope and Instruments V*, SPIE **3356**, 98-105, Kona, Hawaii, 1998
2. F. Zamkotsian, K. Dohlen, D. Burgarella, V. Buat, "Aspects of MMA for MOS: optical modeling and surface characterization, spectrograph optical design", in *Proceedings of the NASA conference on "NGST Science and Technology Exposition"*, ASP Conf. Ser. **207**, 218-224, Hyannis, USA, 1999
3. M. Robberto, A. Cimatti, A. Jacobsen, F. Zamkotsian, F. M. Zerbi, "Applications of DMDs for Astrophysical Research", in *Proceedings of the SPIE conference on MOEMS 2009*, Proc. SPIE **7210**, San Jose, USA (2009)
4. H. Moseley, S. Aslam, M. Baylor, K. Blumenstock, R. Boucarut, A. Erwin, R. Fettig, D. Franz, T. Hadjimichael, J. Hein, A. Kutyrev, M. Li, D. Mott, C. Monroy, D. Schwinger "Microshutter arrays for the NGST NIRSpec", in *Proceedings of the SPIE conference on Astronomical Telescopes and Instrumentation 2002*, Proc. SPIE **4850**, Hawaii, USA, 2002
5. S. Waldis, F. Zamkotsian, P. Lanzoni, W. Noell, N. de Rooij, "Micromirrors for multiobject spectroscopy: optical and cryogenic characterization", in *Proceedings of the SPIE conference on MOEMS 2008*, Proc. SPIE **6887**, San Jose, USA (2008)
6. M. Canonica, S. Waldis, F. Zamkotsian, P. Lanzoni, W. Noell, N. de Rooij, " Development of MEMS-based programmable slit mask for multi-object spectroscopy ", in *Proceedings of the SPIE conference on Astronomical Telescopes and Instrumentation*, Proc. SPIE **7739**, San Diego, USA (2010)
7. F. Zamkotsian, K. Dohlen, "Performance modeling of JWST Near Infrared Multi-Object Spectrograph," in *Proceedings of the SPIE conference on Astronomical Telescopes and Instrumentation 2004*, Proc. SPIE **5487**, Glasgow, United Kingdom (2004)
8. F. Zamkotsian, J. Gautier, P. Lanzoni, "Characterization of MOEMS devices for the instrumentation of Next Generation Space Telescope," in *Proceedings of the SPIE conference on MOEMS 2003*, Proc. SPIE **4980**, San Jose, USA (2003)
9. F. Zamkotsian and K. Dohlen, "Surface characterization of micro-optical components by Foucault's knife-edge method: the case of a micro-mirror array", Applied Optics, **38** (31), 6532-6539 (1999)
10. A. Liotard, F. Zamkotsian, "Static and dynamic micro-deformable mirror characterization by phase-shifting and time-averaged interferometry", in *Proceedings of the SPIE conference on Astronomical Telescopes and Instrumentation 2004*, Proc. SPIE **5494**, Glasgow, United Kingdom (2004)
11. F. Zamkotsian, E. Grassi, P. Lanzoni, R. Barette, C. Fabron, K. Tangen, L. Marchand, L. Duvet "DMD chip space evaluation for ESA EUCLID mission," in *Proceedings of the SPIE conference on MOEMS 2010*, Proc. SPIE **7596**, San Francisco, USA (2010)